[47] Seregin SV, Tumanova I, Petrova ID, Iashina LN, Kuzina II, Vyshemirskii OI, et al. Genomic S segment of Crimean–Congo hemorrhagic fever virus circulating in Russia and Bulgaria. Vopr Virusol 2006;51(3):25–32.
[48] Burt FJ, Swanepoel R. Molecular epidemiology of African and Asian Crimean–Congo haemorrhagic fever isolates. Epidemiol Infect 2005;133(4):659–66.
[49] Petrova ID, Seregin SV, Petrov VS, Vyshemirskii OI, Kuzina II, L'Vov DK, et al. Genetic characteristics of the S-segment of RNA from two strains of the Crimean–Congo hemorrhagic fever virus isolated in the south of Russia and in Uzbekistan. Vopr Virusol 2003;48(2):8–11.
[50] Iashina LN, Petrov VS, Vyshemirskii OI, Aristova VA, Moskvina TM, L'Vov D K, et al. Characteristics of Crimean–Congo hemorrhagic fever virus circulating in Russia and Central Asia. Vopr Virusol 2002;47(3):11–5.
[51] Papa A, Bino S, Llagami A, Brahimaj B, Papadimitriou E, Pavlidou V, et al. Crimean–Congo hemorrhagic fever in Albania, 2001. Eur J Clin Microbiol Infect Dis 2002;21(8):603–6.
[52] Karti SS, Odabasi Z, Korten V, Yilmaz M, Sonmez M, Caylan R, et al. Crimean–Congo hemorrhagic fever in Turkey. Emerg Infect Dis 2004;10(8):1379–84.
[53] Drosten C, Minnak D, Emmerich P, Schmitz H, Reinicke T. Crimean–Congo hemorrhagic fever in Kosovo. J Clin Microbiol 2002;40(3):1122–3.
[54] Hewson R, Chamberlain J, Mioulet V, Lloyd G, Jamil B, Hasan R, et al. Crimean–Congo haemorrhagic fever virus: sequence analysis of the small RNA segments from a collection of viruses world wide. Virus Res 2004;102(2):185–9.
[55] Deyde VM, Khristova ML, Rollin PE, Ksiazek TG, Nichol ST. Crimean-Congo hemorrhagic fever virus genomics and global diversity. J virol 2006;80(17):8834–42.
[56] Chare ER, Gould EA, Holmes EC. Phylogenetic analysis reveals a low rate of homologous recombination in negative-sense RNA viruses. J Gen Virol 2003;84(Pt 10):2691–703.
[57] Lukashev AN. Evidence for recombination in Crimean–Congo hemorrhagic fever virus. J Gen Virol 2005;86(Pt 8):2333–8.
[58] Antoniadis A, Casals J. Serological evidence of human infection with Congo–Crimean hemorrhagic fever virus in Greece. Am J Trop Med Hyg 1982;31(5):1066–7.
[59] Papa A, Christova I, Papadimitriou E, Antoniadis A. Crimean–Congo hemorrhagic fever in Bulgaria. Emerg Infect Dis 2004;10(8):1465–7.
[60] Hewson R, Gmyl A, Gmyl L, Smirnova SE, Karganova G, Jamil B, et al. Evidence of segment reassortment in Crimean–Congo haemorrhagic fever virus. J Gen Virol 2004;85(Pt 10):3059–70.
[61] Yashina L, Vyshemirskii O, Seregin S, Petrova I, Samokhvalov E, Lvov D, et al. Genetic analysis of Crimean-Congo hemorrhagic fever virus in Russia. J Clin Microbiol 2003;41(2):860–2.
[62] Ma B, Hang C, Papa A. Sequencing and comparative analysis of the complete glycoprotein gene of three Crimean–Congo hemorrhagic fever virus Chinese isolates. Zhonghua Shi Yan He Lin Chuang Bing Du Xue Za Zhi 2001;15(2):105–11.
[63] Papa A, Ma B, Kouidou S, Tang Q, Hang C, Antoniadis A. Genetic characterization of the M RNA segment of Crimean Congo hemorrhagic fever virus strains, China. Emerg Infect Dis 2002;8(1):50–3.
[64] Meissner JD, Seregin SS, Seregin SV, Vyshemirskii OI, Yakimenko NV, Netesov SV, et al. The complete genomic sequence of strain ROS/HUVLV-100, a representative Russian Crimean Congo hemorrhagic fever virus strain. Virus Genes 2006;33(1):87–93.
[65] Papa A, Papadimitriou E, Bozovic B, Antoniadis A. Genetic characterization of the M RNA segment of a Balkan Crimean–Congo hemorrhagic fever virus strain. J Med Virol 2005;75(3):466–9.
[66] Seregin SV, Samokhvalov EI, Petrova ID, Vyshemirskii OI, Samokhvalova EG, Lvov DK, et al. Genetic characterization of the M RNA segment of Crimean–Congo hemorrhagic fever virus strains isolated in Russia and Tajikistan. Virus Genes 2004;28(2):187–93.
[67] Chamberlain J, Cook N, Lloyd G, Mioulet V, Tolley H, Hewson R. Co-evolutionary patterns of variation in small and large RNA segments of Crimean–Congo hemorrhagic fever virus. J Gen Virol 2005;86(Pt 12):3337–41.
[68] Burt FJ, Leman PA, Smith JF, Swanepoel R. The use of a reverse transcription-polymerase chain reaction for the detection of viral nucleic acid in the diagnosis of Crimean–Congo haemorrhagic fever. J Virol Methods 1998;70(2):129–37.

Please cite this article as: Morikawa S, et al. Recent progress in molecular biology of Crimean–Congo hemorrhagic.... Comparat Immunol Microbiol Infect Dis. (2007), doi:10.1016/j.cimid.2007.07.001

[69] Duh D, Saksida A, Petrovec M, Dedushaj I, Avsic-Zupanc T. Novel one-step real-time RT-PCR assay for rapid and specific diagnosis of Crimean–Congo hemorrhagic fever encountered in the Balkans. J Virol Methods 2006;133(2):175–9.
[70] Yapar M, Aydogan H, Pahsa A, Besirbellioglu BA, Bodur H, Basustaoglu AC, et al. Rapid and quantitative detection of Crimean–Congo hemorrhagic fever virus by one-step real-time reverse transcriptase-PCR. Jpn J Infect Dis 2005;58(6):358–62.
[71] Drosten C, Kummerer BM, Schmitz H, Gunther S. Molecular diagnostics of viral hemorrhagic fevers. Antivi Res 2003;57(1-2):61–87.
[72] Saijo M, Qing T, Niikura M, Maeda A, Ikegami T, Sakai K, et al. Immunofluorescence technique using HeLa cells expressing recombinant nucleoprotein for detection of immunoglobulin G antibodies to Crimean–Congo hemorrhagic fever virus. J Clin Microbiol 2002;40(2): 372–5.
[73] Saijo M, Qing T, Niikura M, Maeda A, Ikegami T, Prehaud C, et al. Recombinant nucleoprotein-based enzyme-linked immunosorbent assay for detection of immunoglobulin G antibodies to Crimean–Congo hemorrhagic fever virus. J Clin Microbiol 2002;40(5):1587–91.
[74] Drosten C, Gottig S, Schilling S, Asper M, Panning M, Schmitz H, et al. Rapid detection and quantification of RNA of Ebola and Marburg viruses, Lassa virus, Crimean–Congo hemorrhagic fever virus, Rift Valley fever virus, dengue virus, and yellow fever virus by real-time reverse transcription-PCR. J Clin Microbiol 2002;40(7):2323–30.
[75] Saijo M, Tang Q, Shimayi B, Han L, Zhang Y, Asiguma M, et al. Antigen-capture enzyme-linked immunosorbent assay for the diagnosis of Crimean–Congo hemorrhagic fever using a novel monoclonal antibody. J Med Virol 2005;77(1):83–8.
[76] Garcia S, Chinikar S, Coudrier D, Billecocq A, Hooshmand B, Crance JM, et al. Evaluation of a Crimean–Congo hemorrhagic fever virus recombinant antigen expressed by Semliki Forest suicide virus for IgM and IgG antibody detection in human and animal sera collected in Iran. J Clin Virol 2006;35(2):154–9.
[77] Saijo M, Tang Q, Shimayi B, Han L, Zhang Y, Asiguma M, et al. Recombinant nucleoprotein-based serological diagnosis of Crimean–Congo hemorrhagic fever virus infections. J Med Virol 2005;75(2):295–9.
[78] Tang Q, Saijo M, Zhang Y, Asiguma M, Tianshu D, Han L, et al. A patient with Crimean–Congo hemorrhagic fever serologically diagnosed by recombinant nucleoprotein-based antibody detection systems. Clin Diagn Lab Immunol 2003;10(3):489–91.
[79] Marriott AC, Polyzoni T, Antoniadis A, Nuttall PA. Detection of human antibodies to Crimean–Congo haemorrhagic fever virus using expressed viral nucleocapsid protein. J Gen Virol 1994;75(Pt 9):2157–61.
[80] Burt FJ, Leman PA, Abbott JC, Swanepoel R. Serodiagnosis of Crimean–Congo haemorrhagic fever. Epidemiol Infect 1994;113(3):551–62.
[81] Shepherd AJ, Swanepoel R, Gill DE. Evaluation of enzyme-linked immunosorbent assay and reversed passive hemagglutination for detection of Crimean–Congo hemorrhagic fever virus antigen. J Clin Microbiol 1988;26(2):347–53.
[82] Saluzzo JF, Le Guenno B. Rapid diagnosis of human Crimean–Congo hemorrhagic fever and detection of the virus in naturally infected ticks. J Clin Microbiol 1987;25(5):922–4.
[83] Watts DM, Ussery MA, Nash D, Peters CJ. Inhibition of Crimean–Congo hemorrhagic fever viral infectivity yields in vitro by ribavirin. Am J Trop Med Hyg 1989;41(5):581–5.
[84] Paragas J, Whitehouse CA, Endy TP, Bray M. A simple assay for determining antiviral activity against Crimean–Congo hemorrhagic fever virus. Antiviral Res 2004;62(1):21–5.
[85] Tignor GH, Hanham CA. Ribavirin efficacy in an in vivo model of Crimean–Congo hemorrhagic fever virus (CCHF) infection. Antiviral Res 1993;22(4):309–25.
[86] Fisher-Hoch SP, Khan JA, Rehman S, Mirza S, Khurshid M, McCormick JB. Crimean Congo–haemorrhagic fever treated with oral ribavirin. Lancet 1995;346(8973):472–5.
[87] Ozkurt Z, Kiki I, Erol S, Erdem F, Yilmaz N, Parlak M, et al. Crimean–Congo hemorrhagic fever in Eastern Turkey: clinical features, risk factors and efficacy of ribavirin therapy. J Infect 2006;52(3): 207–15.

Please cite this article as: Morikawa S, et al. Recent progress in molecular biology of Crimean–Congo hemorrhagic.... Comparat Immunol Microbiol Infect Dis. (2007), doi:10.1016/j.cimid.2007.07.001

[88] Jabbari A, Besharat S, Abbasi A, Moradi A, Kalavi K. Crimean–Congo hemorrhagic fever: case series from a medical center in Golestan province, Northeast of Iran (2004). Indian J Med Sci 2006; 60(8):327–9.
[89] Ergonul O, Celikbas A, Baykam N, Eren S, Dokuzoguz B. Analysis of risk-factors among patients with Crimean–Congo haemorrhagic fever virus infection: severity criteria revisited. Clin Microbiol Infect 2006;12(6):551–4.
[90] Bakir M, Ugurlu M, Dokuzoguz B, Bodur H, Tasyaran MA, Vahaboglu H. Crimean–Congo haemorrhagic fever outbreak in Middle Anatolia: a multicentre study of clinical features and outcome measures. J Med Microbiol 2005;54(Pt 4):385–9.
[91] Ergonul O, Celikbas A, Dokuzoguz B, Eren S, Baykam N, Esener H. Characteristics of patients with Crimean–Congo hemorrhagic fever in a recent outbreak in Turkey and impact of oral ribavirin therapy. Clin Infect Dis 2004;39(2):284–7.
[92] Mardani M, Jahromi MK, Naieni KH, Zeinali M. The efficacy of oral ribavirin in the treatment of Crimean–Congo hemorrhagic fever in Iran. Clin Infect Dis 2003;36(12):1613–8.
[93] Spik K, Shurtleff A, McElroy AK, Guttieri MC, Hooper JW, SchmalJohn C. Immunogenicity of combination DNA vaccines for Rift Valley fever virus, tick-borne encephalitis virus, Hantaan virus, and Crimean Congo hemorrhagic fever virus. Vaccine 2006;24(21):4657–66.

Please cite this article as: Morikawa S, et al. Recent progress in molecular biology of Crimean–Congo hemorrhagic.... Comparat Immunol Microbiol Infect Dis. (2007), doi:10.1016/j.cimid.2007.07.001

JOURNAL OF VIROLOGY, Oct. 2007, p. 10831–10834
0022-538X/07/$08.00+0 doi:10.1128/JVI.01143-07

Vol. 81, No. 19

Amino Acid Substitutions in the S2 Region Enhance Severe Acute Respiratory Syndrome Coronavirus Infectivity in Rat Angiotensin-Converting Enzyme 2-Expressing Cells[▽]

Shuetsu Fukushi,[1]* Tetsuya Mizutani,[1] Kouji Sakai,[1] Masayuki Saijo,[1] Fumihiro Taguchi,[2] Masaru Yokoyama,[3] Ichiro Kurane,[1] and Shigeru Morikawa[1]

Department of Virology I,[1] Department of Virology III,[2] and Center for Pathogen Genomics,[3] National Institute of Infectious Diseases, Gakuen 4-7-1, Musashimurayama, Tokyo 208-0011, Japan

Received 25 May 2007/Accepted 16 July 2007

To clarify the molecular basis of severe acute respiratory syndrome coronavirus (SARS-CoV) adaptation to different host species, we serially passaged SARS-CoV in rat angiotensin-converting enzyme 2 (ACE2)-expressing cells. After 15 passages, the virus (Rat-P15) came to replicate effectively in rat ACE2-expressing cells. Two amino acid substitutions in the S2 region were found on the Rat-P15 S gene. Analyses of the infectivity of the pseudotype-bearing S protein indicated that the two substitutions in the S2 region, especially the S950F substitution, were responsible for efficient infection. Therefore, virus adaptation to different host species can be induced by amino acid substitutions in the S2 region.

The 2002 to 2003 epidemic of severe acute respiratory syndrome (SARS) was caused by SARS coronavirus (SARS-CoV) infection. Initially, SARS-CoV was thought to be transmitted first from marketplace animals to humans and then by human-to-human spread (3, 7, 8). Although marketplace animals may be the immediate source of the SARS-CoV found in humans, SARS-CoV has been detected in other wild animals, e.g., civet cats, raccoon dogs (7), ferrets, and cats (15), suggesting that SARS-CoV may have a broad host range. In addition, rats are suggested to have been an animal vector in the SARS outbreak in the Amoy Gardens in Hong Kong (20). Recently, horseshoe bats have been reported to be a natural reservoir of coronaviruses close to SARS-CoV, and it is suggested that bats are candidate natural reservoirs of SARS-CoV (9, 13). In order to understand how the virus jumped to humans, it is important to elucidate the molecular mechanism of SARS-CoV adaptation to different species.

The SARS-CoV S protein mediates virus entry into cells expressing the receptor molecule angiotensin-converting enzyme 2 (ACE2) (12). The receptor binding domain (RBD), located on the S1 region, is believed to be the critical determinant of virus-receptor interaction (10, 27). It has been shown that amino acid substitutions on the RBD are associated with the SARS-CoV from palm civets adapted to humans (14). Furthermore, a single amino acid substitution on the RBD caused by serial in vivo passage of SARS-CoV in rats was strongly associated with increased infection of rat ACE2-expressing cells (18). Thus, substitution(s) of amino acid residues on the RBD may be one of the critical molecular determinants of SARS-CoV adaptation. On the other hand, in the case of mouse hepatitis virus, one or more amino acid substitutions of the S2 region, in combination with those of the S1 region, are intimately involved in receptor binding and extended host range (2, 16, 19). The presence of a neutralizing epitope within the S2 region of the SARS-CoV suggests that the S protein binding to the host cell surface not only relies on the S1 region but also depends on the global protein structure, including the S2 region (4, 28, 29). These studies suggested that several factors, including amino acid substitutions in the S2 region, in addition to those in the RBD in the S1 region, play roles in determining SARS-CoV infectivity. Thus, analyses of the entire amino acid sequence of the S protein may be necessary to understand the molecular mechanisms of viral adaptation to different species.

Notably, SARS-CoV S protein-mediated entry into cells expressing rat ACE2 has been shown to be extremely low (11, 14). Since the coronavirus serially passaged in vitro acquires amino acid substitutions that might be relevant to virus adaptation to different types of cells (5, 23), we speculated that in vitro passage of SARS-CoV in cells expressing species-specific ACE2 would induce viral adaptation to different animal species. To examine SARS-CoV adaptation to rat ACE2, we compared replication efficiencies for SARS-CoV serially passaged in rat ACE2-expressing cells and for a parental SARS-CoV strain when inoculated to cells expressing rat ACE2.

The SARS-CoV Frankfurt-1 strain was inoculated at a multiplicity of infection (MOI) of 0.01 PFU/cell onto Chinese hamster ovary (CHO) cells transiently transfected with the expression plasmid pcDNArat ACE2, which encodes rat ACE2 (18). The expression of ACE2 proteins was confirmed by Western blotting (Fig. 1A). The plasmids were transfected into the CHO cells at efficiencies of about 80%, as estimated by indirect immunofluorescence methods (data not shown). The virus, which was obtained from the culture supernatants of Frankfurt-1-infected rat ACE2-expressing CHO cells, was reinoculated at an MOI of 0.01 PFU/cell onto fresh CHO cells expressing rat ACE2. The culture supernatants were collected

* Corresponding author. Mailing address: Special Pathogens Laboratory, Department of Virology I, National Institute of Infectious Diseases, Gakuen 4-7-1, Musashimurayama, Tokyo 208-0011, Japan. Phone: 81-42-561-0771. Fax: 81-42-564-4881. E-mail: fukushi@nih.go.jp.

▽ Published ahead of print on 25 July 2007.

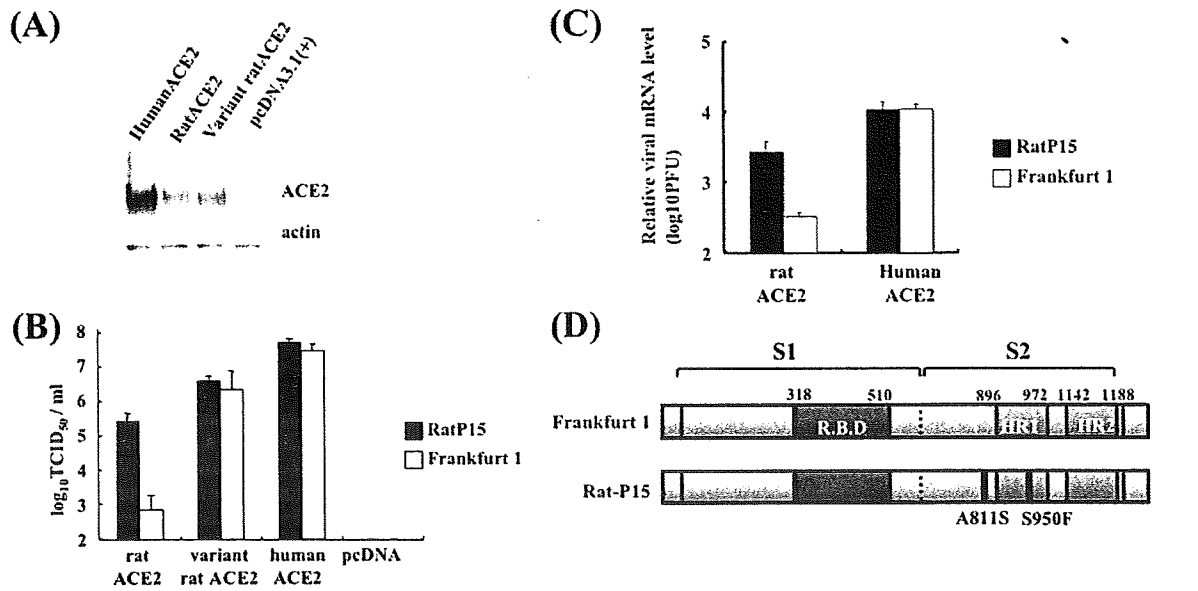

FIG. 1. Comparison of replication efficiencies of the SARS-CoV Rat-P15 strain serially passaged in rat ACE2-expressing cells and that of a parental SARS-CoV strain (Frankfurt-1). (A) Expression of ACE2 proteins. CHO cells were transfected with plasmid pTargeT-hACE2 (6), pcDNArat ACE2, and pcDNArat ACE2MUT2 (18), which encode human ACE2, rat ACE2, and variant rat ACE2 with amino acid residues 82 to 84 (NYS) corresponding to human ACE2 (MYP), respectively. Equal volumes of cell lysates were analyzed by Western blotting using a goat antibody specific for human ACE2 (6) or β-actin. The low signal intensity on rat ACE2 is due to the lower reactivity of the antiserum to rat ACE2. (B) Replication of viruses in CHO cells expressing rat ACE2, variant rat ACE2, or human ACE2. Rat-P15 or a parent Frankfurt-1 strain was inoculated to CHO cells transfected with expression plasmids pcDNArat ACE2, pcDNArat ACE2MUT2, pTargeT-hACE2, or the pcDNA3.1(+) vector. After 72 h, the replications of the virus in the cells were determined as 50% tissue culture infectious doses ($TCID_{50}$)/ml on Vero E6 cells. (C) Assessment of virus entry of Rat-P15 on rat ACE2-expressing cells. CHO cells were transfected with expression plasmids encoding rat ACE2 or human ACE2. After 48 h, 10,000 PFU of Rat-P15 or a parent Frankfurt-1 strain was inoculated. After 5 h, the culture medium was removed, and viral RNAs were isolated from the infected cells. Virus entry efficiency was estimated by quantification of the mRNA9 level with a real-time PCR assay (17). (D) Schematic representation of S proteins of Rat-P15 and Frankfurt 1. Amino acid substitutions at residues 811 and 950 in the S2 region of Rat-P15 are shown. The locations of the RBD, heptad repeat 1 (HR1), and HR2 are shown as filled boxes.

after 48 hours postinfection (hpi). All the following passages were performed by inoculation of the virus at an MOI of 0.002 PFU/cell and by collection of the culture supernatants at 72 hpi. Passages were performed 15 times, and the virus (Rat-P15) was obtained from culture supernatants. In order to examine whether serial passages of SARS-CoV makes the virus replicate efficiently in rat ACE2-expressing cells, Rat-P15 or a parent Frankfurt-1 strain was inoculated onto CHO cells that express rat ACE2. After 72 h, the virus titers of the culture supernatants were determined. The replication of Rat-P15 was higher than that of the parent Frankfurt-1 strain in rat ACE2-expressing CHO cells (Fig. 1B). In contrast, the replication of Rat-P15 was similar to that of parent Frankfurt-1 strain in CHO cells expressing human ACE2 or variant rat ACE2 with amino acid residues 82 to 84 (NYS) corresponding to human ACE2 (MYP) (18) (Fig. 1B). These results indicate that Rat-P15 came to replicate more efficiently in rat ACE2-expressing cells.

To examine whether the Rat-P15 strain acquired the ability to infect rat ACE2-expressing cells more efficiently than the parent Frankfurt-1 strain, viral infection was determined by quantitative real-time PCR assay after a shorter incubation period (17). Viruses were inoculated onto CHO cells expressing rat ACE2 or human ACE2. After 5 h, virus entry was estimated by measuring the amounts of newly synthesized mRNA9 of SARS-CoV. As shown in Fig. 1C, Rat-P15 propagated more efficiently than Frankfurt-1 strain in rat ACE2-expressing CHO cells by more than 10-fold. This result indicates that serial passages of SARS-CoV in rat ACE2-expressing cells efficiently increased its ability to infect rat ACE2-expressing cells.

To examine whether the Rat-P15 strain acquired amino acid substitutions within the S protein during serial passage, the nucleotide sequence of the S gene was determined as described previously (18). Interestingly, the amino acid sequence of the RBD of Rat-P15 was identical to that of the parent Frankfurt-1 strain. In contrast, two amino acid substitutions on the S2 region were found: serine for alanine at amino acid position 811 (A811S) and phenylalanine for serine at position 950 (S950F) (Fig. 1D). Nucleotide sequencing of this region at passages 1, 3, 5, 7, 9, 11, and 13 revealed that A811S substitution occurred after the 11th passage on rat ACE2-expressing cells, whereas the S950F substitution occurred after the 3rd passage (data not shown). This suggests that the two amino acid substitutions had distinct roles in enhancing viral infection in rat ACE2-expressing cells. On the other hand, virus which was passaged 11 times in cells expressing variant rat ACE2 did not have any amino acid substitutions in the S protein. These results suggest that A811S and S950F substitutions were not solely dependent on infection of CHO cells but were triggered by serial passage in rat ACE2-expressing CHO cells.

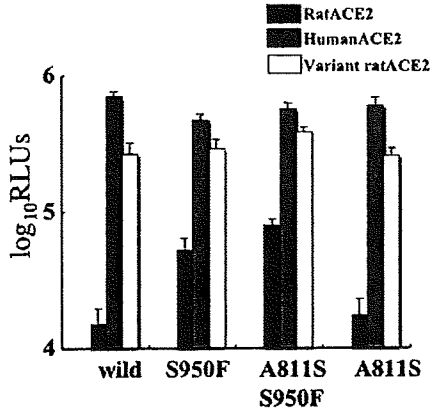

FIG. 2. Analysis of the significance of amino acid substitutions in the S2 region for the efficient entry of the virus into rat ACE2-expressing cells; analysis was done using VSV pseudotypes. VSVΔG*/SEAP-G, in which the VSV glycoprotein gene was replaced with the SEAP (*se*creted-type *a*lkaline *p*hosphatase) gene, was used for generating VSV pseudotypes bearing the C-terminally truncated S protein of SARS-CoV as described previously (6). BHK cells expressing rat, variant rat, or human ACE2 were inoculated with approximately 10^3 infectious units of VSV-St19 (wild), VSV-St19-A811S (A811S), VSV-St19-S950F (S950F), or VSV-St19-A811S-S950F (A811S S950F). At 18 hpi, SEAP activities of culture supernatants were measured by intensities of chemiluminescence reactions of alkaline phosphatase and are represented as relative luminescence units (RLUs). The VSV pseudotype bearing the S950F substitution rather than the A811S substitution efficiently infected rat ACE2-expressing cells.

In order to analyze the significance of the two amino acid substitutions for the efficient entry of the virus to rat ACE2-expressing cells, a vesicular stomatitis virus (VSV) pseudotyping system (kindly provided by M. A. Whitt) (6) was employed. VSV pseudotypes bearing S protein with a single amino acid substitution (VSV-St19-A811S and VSV-St19-S950F), bearing that with A811S and S950F double amino acid substitutions (VSV-St19-A811S-S950F), and bearing that having the amino acids of the wild type (VSV-St19) were generated. After the expression plasmids encoding rat ACE2, variant rat ACE2, and human ACE2 were transfected to Syrian baby hamster kidney (BHK) cells, each VSV pseudotype was inoculated. All the VSV pseudotypes infected human ACE2- or variant rat ACE2-expressing cells at similar levels (Fig. 2). On the other hand, VSV-St19-A811S-S950F infected rat ACE2-expressing cells more efficiently than VSV-St19. Interestingly, VSV-St19-S950F, which carries the S protein with the S950F substitution, infected rat ACE2-expressing cells more efficiently than did VSV-St19-A811S with the A811S substitution or VSV-St19. This indicates that the S950F substitution has a significant role in the efficient entry mediated by rat ACE2.

It has been shown that a single amino acid substitution in the S2 region affects the maturation of the glycosylation process of SARS-CoV S protein (1). Several lines of evidence indicate that glycosylation of viral envelope proteins is a molecular determinant for virus replication and infectivity (22, 24, 25, 26). Therefore, the wild-type and mutant S proteins were subjected to Western blotting to investigate the effect of the amino acid substitutions on the glycosylation of the S protein. The mutant S protein with a single A811S substitution (S-A811S), as well as the wild-type S protein (S-wt), migrated somewhat more slowly than those with a single S950F substitution (S-S950F) or with A811S and S950F substitutions (S-A811S-S950F) (Fig. 3). When S proteins were digested with endo-H, all mutant proteins migrated with molecular masses comparable to those of undigested controls. In contrast, when the expressed S proteins were digested with PNGase-F, all the mutant proteins showed migration patterns similar to that of the wild-type S protein. This indicates that differences in migration patterns of S-S950F and S-A811S-S950F were due to altered attachment of complex oligosaccharides during maturation. Our results indicate that S950F substitution affected N-linked glycosylation of the S protein and suggest that these differences are well correlated with the increased efficiency of SARS-CoV infection of rat ACE2-expressing cells.

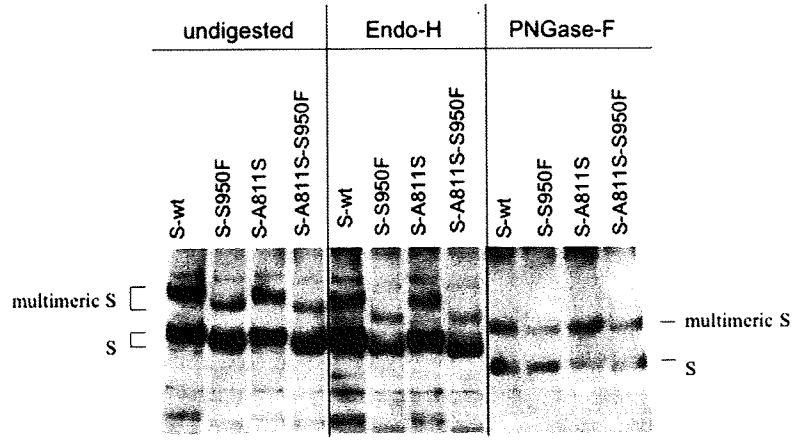

FIG. 3. Analysis of N-linked glycosylation of S proteins. SARS-CoV S proteins with the wild-type sequence (S-wt), an S950F substitution (S-S950F), an A811S substitution (S-A811S), and A811S and S950F substitutions (S-A811S-S950F) that were expressed in 293T cells were treated with endo-H or PNGase-F and then subjected along with undigested samples to sodium dodecyl sulfate-polyacrylamide gel electrophoresis. The S protein was detected by Western blotting using a rabbit antibody specific for the S2 region (6).

In contrast to our findings that amino acid substitutions were found in the S2 region, a substitution of tyrosine by serine located in the RBD was detected in the in vivo-adapted SARS-CoV (18). The difference between in vivo and in vitro passage may be attributed to replication sites; the substitution on the RBD seems to be responsible for the efficient replication of the virus on the alveolar area, where ACE2 is expressed at a low level (18), whereas virus replicated in CHO cells where ACE2 was abundantly expressed by transfection of expression plasmids. Alternatively, it seems likely that innate immune responses in rats could select a particular SARS-CoV strain adapted to rats. In summary, SARS-CoV adaptation to a particular animal species can be induced by amino acid substitutions in the RBD within the S1 region but also by those in the S2 region.

We thank J. Ziebuhr of the Institute of Virology and Immunology, University of Wurzburg, Wurzburg, Germany, for providing SARS-CoV Frankfurt-1 isolate and M. A. Whitt of GTx, Inc., for providing VSVΔG*/SEAP-G. We also thank M. Ogata for her assistance.

This work was supported in part by a grant-in-aid from the Ministry of Health, Labor, and Welfare of Japan and the Japan Society for the Promotion of Science.

REFERENCES

1. **Chan, W. E., C. K. Chuang, S. H. Yeh, M. S. Chang, and S. S. Chen.** 2006. Functional characterization of heptad repeat 1 and 2 mutants of the spike protein of severe acute respiratory syndrome coronavirus. J. Virol. **80:**3225–3237.
2. **de Haan, C. A., E. Te Lintelo, Z. Li, M. Raaben, T. Wurdinger, B. J. Bosch, and P. J. Rottier.** 2006. Cooperative involvement of the S1 and S2 subunits of the murine coronavirus spike protein in receptor binding and extended host range. J. Virol. **80:**10909–10918.
3. **Drosten, C., S. Gunther, W. Preiser, S. van der Werf, H. R. Brodt, S. Becker, H. Rabenau, M. Panning, L. Kolesnikova, R. A. Fouchier, A. Berger, A. M. Burguiere, J. Cinatl, M. Eickmann, N. Escriou, K. Grywna, S. Kramme, J. C. Manuguerra, S. Muller, V. Rickerts, M. Sturmer, S. Vieth, H. D. Klenk, A. D. Osterhaus, H. Schmitz, and H. W. Doerr.** 2003. Identification of a novel coronavirus in patients with severe acute respiratory syndrome. N. Engl. J. Med. **348:**1967–1976.
4. **Duan, J., X. Yan, X. Guo, W. Cao, W. Han, C. Qi, J. Feng, D. Yang, G. Gao, and G. Jin.** 2005. A human SARS-CoV neutralizing antibody against epitope on S2 protein. Biochem. Biophys. Res. Commun. **333:**186–193.
5. **Fang, S. G., S. Shen, F. P. Tay, and D. X. Liu.** 2005. Selection of and recombination between minor variants lead to the adaptation of an avian coronavirus to primate cells. Biochem. Biophys. Res. Commun. **336:**417–423.
6. **Fukushi, S., T. Mizutani, M. Saijo, S. Matsuyama, N. Miyajima, F. Taguchi, S. Itamura, I. Kurane, and S. Morikawa.** 2005. Vesicular stomatitis virus pseudotyped with severe acute respiratory syndrome coronavirus spike protein. J. Gen. Virol. **86:**2269–2274.
7. **Guan, Y., B. J. Zheng, Y. Q. He, X. L. Liu, Z. X. Zhuang, C. L. Cheung, S. W. Luo, P. H. Li, L. J. Zhang, Y. J. Guan, K. M. Butt, K. L. Wong, K. W. Chan, W. Lim, K. F. Shortridge, K. Y. Yuen, J. S. Peiris, and L. L. Poon.** 2003. Isolation and characterization of viruses related to the SARS coronavirus from animals in southern China. Science **302:**276–278.
8. **Ksiazek, T. G., D. Erdman, C. S. Goldsmith, S. R. Zaki, T. Peret, S. Emery, S. Tong, C. Urbani, J. A. Comer, W. Lim, P. E. Rollin, S. F. Dowell, A. E. Ling, C. D. Humphrey, W. J. Shieh, J. Guarner, C. D. Paddock, P. Rota, B. Fields, J. DeRisi, J. Y. Yang, N. Cox, J. M. Hughes, J. W. LeDuc, W. J. Bellini, and L. J. Anderson.** 2003. A novel coronavirus associated with severe acute respiratory syndrome. N. Engl. J. Med. **348:**1953–1966.
9. **Lau, S. K., P. C. Woo, K. S. Li, Y. Huang, H. W. Tsoi, B. H. Wong, S. S. Wong, S. Y. Leung, K. H. Chan, and K. Y. Yuen.** 2005. Severe acute respiratory syndrome coronavirus-like virus in Chinese horseshoe bats. Proc. Natl. Acad. Sci. USA **102:**14040–14045.
10. **Li, F., W. Li, M. Farzan, and S. C. Harrison.** 2005. Structure of SARS coronavirus spike receptor-binding domain complexed with receptor. Science **309:**1864–1868.
11. **Li, W., T. C. Greenough, M. J. Moore, N. Vasilieva, M. Somasundaran, J. L. Sullivan, M. Farzan, and H. Choe.** 2004. Efficient replication of severe acute respiratory syndrome coronavirus in mouse cells is limited by murine angiotensin-converting enzyme 2. J. Virol. **78:**11429–11433.
12. **Li, W., M. J. Moore, N. Vasilieva, J. Sui, S. K. Wong, M. A. Berne, M. Somasundaran, J. L. Sullivan, K. Luzuriaga, T. C. Greenough, H. Choe, and M. Farzan.** 2003. Angiotensin-converting enzyme 2 is a functional receptor for the SARS coronavirus. Nature **426:**450–454.
13. **Li, W., Z. Shi, M. Yu, W. Ren, C. Smith, J. H. Epstein, H. Wang, G. Crameri, Z. Hu, H. Zhang, J. Zhang, J. McEachern, H. Field, P. Daszak, B. T. Eaton, S. Zhang, and L. F. Wang.** 2005. Bats are natural reservoirs of SARS-like coronaviruses. Science **310:**676–679.
14. **Li, W., C. Zhang, J. Sui, J. H. Kuhn, M. J. Moore, S. Luo, S. K. Wong, I. C. Huang, K. Xu, N. Vasilieva, A. Murakami, Y. He, W. A. Marasco, Y. Guan, H. Choe, and M. Farzan.** 2005. Receptor and viral determinants of SARS-coronavirus adaptation to human ACE2. EMBO J. **24:**1634–1643.
15. **Martina, B. E., B. L. Haagmans, T. Kuiken, R. A. Fouchier, G. F. Rimmelzwaan, G. Van Amerongen, J. S. Peiris, W. Lim, and A. D. Osterhaus.** 2003. Virology: SARS virus infection of cats and ferrets. Nature **425:**915.
16. **Matsuyama, S., and F. Taguchi.** 2002. Communication between S1N330 and a region in S2 of murine coronavirus spike protein is important for virus entry into cells expressing CEACAM1b receptor. Virology **295:**160–171.
17. **Matsuyama, S., M. Ujike, S. Morikawa, M. Tashiro, and F. Taguchi.** 2005. Protease-mediated enhancement of severe acute respiratory syndrome coronavirus infection. Proc. Natl. Acad. Sci. USA **102:**12543–12547.
18. **Nagata, N., N. Iwata, H. Hasegawa, S. Fukushi, M. Yokoyama, A. Harashima, Y. Sato, M. Saijo, S. Morikawa, and T. Sata.** 2007. Participation of both host and virus factors in induction of severe acute respiratory syndrome (SARS) in F344 rats infected with SARS coronavirus. J. Virol. **81:**1848–1857.
19. **Navas-Martin, S., S. T. Hingley, and S. R. Weiss.** 2005. Murine coronavirus evolution in vivo: functional compensation of a detrimental amino acid substitution in the receptor binding domain of the spike glycoprotein. J. Virol. **79:**7629–7640.
20. **Ng, S. K.** 2003. Possible role of an animal vector in the SARS outbreak at Amoy Gardens. Lancet **362:**570–572.
21. Reference deleted.
22. **Pikora, C., C. Wittish, and R. C. Desrosiers.** 2005. Identification of two N-linked glycosylation sites within the core of the simian immunodeficiency virus glycoprotein whose removal enhances sensitivity to soluble CD4. J. Virol. **79:**12575–12583.
23. **Poon, L. L., C. S. Leung, K. H. Chan, K. Y. Yuen, Y. Guan, and J. S. Peiris.** 2005. Recurrent mutations associated with isolation and passage of SARS coronavirus in cells from non-human primates. J. Med. Virol. **76:**435–440.
24. **Scherret, J. H., J. S. Mackenzie, A. A. Khromykh, and R. A. Hall.** 2001. Biological significance of glycosylation of the envelope protein of Kunjin virus. Ann. N. Y. Acad. Sci. **951:**361–363.
25. **Shi, X., K. Brauburger, and R. M. Elliott.** 2005. Role of N-linked glycans on Bunyamwera virus glycoproteins in intracellular trafficking, protein folding, and virus infectivity. J. Virol. **79:**13725–13734.
26. **Shirato, K., H. Miyoshi, A. Goto, Y. Ako, T. Ueki, H. Kariwa, and I. Takashima.** 2004. Viral envelope protein glycosylation is a molecular determinant of the neuroinvasiveness of the New York strain of West Nile virus. J. Gen. Virol. **85:**3637–3645.
27. **Wong, S. K., W. Li, M. J. Moore, H. Choe, and M. Farzan.** 2004. A 193-amino acid fragment of the SARS coronavirus S protein efficiently binds angiotensin-converting enzyme 2. J. Biol. Chem. **279:**3197–3201.
28. **Zeng, F., C. C. Hon, C. W. Yip, K. M. Law, Y. S. Yeung, K. H. Chan, J. S. Malik Peiris, and F. C. Leung.** 2006. Quantitative comparison of the efficiency of antibodies against S1 and S2 subunit of SARS coronavirus spike protein in virus neutralization and blocking of receptor binding: implications for the functional roles of S2 subunit. FEBS Lett. **580:**5612–5620.
29. **Zhong, X., H. Yang, Z. F. Guo, W. Y. Sin, W. Chen, J. Xu, L. Fu, J. Wu, C. K. Mak, C. S. Cheng, Y. Yang, S. Cao, T. Y. Wong, S. T. Lai, Y. Xie, and Z. Guo.** 2005. B-cell responses in patients who have recovered from severe acute respiratory syndrome target a dominant site in the S2 domain of the surface spike glycoprotein. J. Virol. **79:**3401–3408.

RESEARCH ARTICLE

Phosphorylation of measles virus nucleoprotein upregulates the transcriptional activity of minigenomic RNA

Kyoji Hagiwara[1], Hiroki Sato[1], Yoshihisa Inoue[1], Akira Watanabe[1], Misako Yoneda[1], Fusako Ikeda[1], Kentaro Fujita[1], Hiroyuki Fukuda[2], Chizuko Takamura[2], Hiroko Kozuka-Hata[2, 3], Masaaki Oyama[2, 3], Sumio Sugano[3], Shinobu Ohmi[2] and Chieko Kai[1]

[1] Laboratory Animal Research Center, Graduate School of Frontier Sciences, The Institute of Medical Science, The University of Tokyo, Tokyo, Japan
[2] Medical Proteomics Laboratory, Graduate School of Frontier Sciences, The Institute of Medical Science, The University of Tokyo, Tokyo, Japan
[3] Department of Medical Genome Sciences, Graduate School of Frontier Sciences, The Institute of Medical Science, The University of Tokyo, Tokyo, Japan

We report the first identification of phosphorylation sites of the nucleoprotein (N) of the family *Paramyxoviridae*. The N protein is known to be the most abundant protein in infected cells; it constructs the N–RNA complex (nucleocapsid) and supports transcription and replication of viral genomic RNA. To determine the role of phosphorylation of the N protein, we expressed the N protein of the HL strain of measles virus (MV) in mammalian cells and purified the nucleocapsid. After separation of the C-terminal region from the core region, phosphorylated amino acids were assayed using MALDI-TOF/TOF and ESI-Q-TOF MS analyses. Two amino acids, S479 and S510, were shown to be phosphorylated by both methods of analysis. Metabolic labeling of the N protein with ^{32}P demonstrated that these two sites are the major phosphorylated sites within the MV-N protein. In transcriptional analysis using negative-strand minigenomic RNA containing the ORF of the luciferase gene, mutants of each phosphorylation site showed approximately 80% reduction in luciferase activity compared with the wild-type N, suggesting that the phosphorylation of N protein is important in the activation of the transcription of viral mRNA and/or replication of the genome *in vivo*.

Received: November 14, 2007
Revised: January 5, 2008
Accepted: January 9, 2008

Keywords:
Measles virus / MS/MS analysis / Nucleoprotein / *Paramyxoviridae* / Phosphorylation

1 Introduction

The *Paramyxoviridae* include some of the most important pathogens of human and animals, and comprise five genera containing more than twenty species of viruses [1]. Measles virus (MV), which belongs to the genus *Morbillivirus* in the family *Paramyxoviridae*, causes a highly contagious disease of humans characterized by a prodromal illness of fever, coryza, cough, and conjunctivitis, followed by the appearance of a generalized maculopapular rash. Despite the development of a successful live attenuated vaccine, MV infection remains a major cause of mortality in children, particularly in developing countries, and a cause of repeated outbreaks in industrialized nations [2].

The MV genome is composed of nonsegmented negative-strand RNA, and the virus has six structural proteins: hemagglutinin, fusion protein, matrix protein, nucleoprotein (N), phosphoprotein (P), and large RNA polymerase (L).

Correspondence: Professor Chieko Kai, The Institute of Medical Science, The University of Tokyo, Shirokanedai, Minato-ku, Tokyo 108-8639, Japan
E-mail: ckai@ims.u-tokyo.ac.jp
Fax: +81-3-5449-5379

Abbreviations: EM, electron microscopy; **MV,** measles virus; **RNP,** ribonucleoprotein; **wt,** wild-type

The gene for the P protein produces two other proteins, C and V, by the usage of an alternative initiation codon and by site-specific RNA editing, respectively [3, 4]. Among these proteins, the N protein is most abundantly expressed in infected cells, and binds to viral genomic RNA to construct a large N-RNA complex (nucleocapsid) that has a herringbone structure [2]. When the N protein is expressed alone, it binds nonspecifically to cellular RNA and forms a similar herringbone structure [5]. The major function of the N protein is to surround the genomic RNA and to support replication and transcription, together with the P and L proteins. In the replication cycle of MV, the nucleocapsid, P and L proteins are assembled into the viral replication unit, which is called the ribonucleoprotein (RNP). The P and N proteins are reported to be present as phosphorylated forms that may play an important role in replication and/or transcription [6–10]. However, identification of the phosphorylation sites of viral proteins by mutagenic analysis has been hampered by the presence of many putative phosphorylation sites in their amino acid sequences, thus identification of such sites and their relevance to the function of the protein have been reported rarely. In the present study, we identified phosphorylation sites on the expressed N protein of MV using MALDI-TOF/TOF and ESI-Q-TOF MS, and investigated the effect of phosphorylation of the N protein on viral transcription.

2 Materials and methods

2.1 Cells and viruses

Cos-7and 293 cells were cultured in DMEM (Sigma, USA) containing 100 U/mL of penicillin G, 100 μg/mL of streptomycin (Invitrogen, USA), and 10% FBS (Sigma). COBL-a cells [11] were cultured in RPMI 1640 (Sigma) containing the same concentrations of antibiotics and FBS. The HL strain of MV [12, 13] was propagated in COBL-a cells by the standard method, as described previously [11].

Sf-9 cells were cultured in Grace's Insect Cell Culture Medium (Invitrogen) with the same concentrations of antibiotics and FBS as described above.

2.2 Construction of expression plasmids

The cDNAs corresponding to the ORF of MV-N, L, and P which had been modified so as not to express C protein, were amplified by PCR using the primers Sal-N-F: GCGGTCGACGCCATGGCCACACTTTTGAGGAGC, Not-N-R: GCGCGGCCGCTAGTCTAGAAGATCTCTGTCATTG, Sal-L-F: GCGGTCGACGCCATGGACTCGCTATCTGTCAAC, Not-L-R: GCGCGGCCGCTAATCCTTAATCAGAGCGCTGTATC, Sal-P-F: GCGGTCGACGCCATGGCAGAAGAGCAGGCACGC, and Not-P-R: GCGCGGCCGCTACTTCATTATTATCTTCATCAGC. PCR amplification was performed using a KOD Plus Ver. 2 (Toyobo, Japan) using a full-length cDNA clone of the MV HL strain (pMV 7 + or pMV 7 + PΔC; unpublished data) as a template. After purification of the products using a MinElute PCR Purification Kit (Qiagen, Germany), they were digested using the appropriate restriction enzymes and cloned into the pCAGGS mammalian expression vector [14]. The PCR product of MV-N was also cloned into the pTNT (Promega, USA) and pAcGHLT vectors (BD Biosciences, USA).

2.3 Production of MV-N-specific antibody

The cDNA of MV-N was cloned into pAcGHLT (BD Biosciences) in frame with N-terminal GST and polyhistidine tags. To obtain the recombinant baculovirus, Sf-9 cells were cotransfected with BaculoGold linearized Baculovirus DNA (BD Biosciences) and the expression plasmid pAcGHLT/MV-N. The fusion N protein was expressed in Sf-9 cells infected with the recombinant baculovirus, and purified using Ni-NTA agarose beads (Qiagen) according to the manufacturer's instructions. Antiserum was raised in a rabbit by immunizing with approximately 100 μg of purified fusion N protein mixed with complete Freund's adjuvant (Difco, USA). Serum was collected 3 wk after injection.

2.4 Expression of MV-N protein and purification of nucleocapsid

Cos-7 cells (1.0×10^6 cells) were transfected with 6.0 μg of pCAGGS vector containing the ORF of the MV-N protein of the HL strain using FuGene 6 Transfection Reagent (Roche, USA) in accordance with the manufacturer's instructions. Two days after transfection, cells were lysed in 500 μL of lysis buffer containing 10 mM Tris (pH 7.8), 150 mM NaCl, 1 mM EDTA, and 1% NP-40 at 4°C for 30 min. The lysate was centrifuged at 15 000 rpm for 10 min by high-speed microcentrifuge MX-100 (Tomy, Japan), and the supernatant was layered onto a discontinuous gradient containing 25, 30, and 40% w/w cesium chloride prepared in lysis buffer without NP-40. The gradient was then centrifuged at 55 000 rpm for 30 min in an Optima™ XL-100K Ultracentrifuge with an SW55Ti rotor (Beckman, USA), and the band material that contained the nucleocapsid was collected. Finally, the sample was pelleted by ultracentrifugation at 70 000 rpm for 10 min in an Optima TL Ultracentrifuge with a TLA100.3 rotor (Beckman) and suspended in 50 μL of PBS.

2.5 SDS-PAGE and Western blot analysis

Purified proteins were separated by 10% SDS-PAGE under reducing conditions and stained with CBB. Western blot analysis was performed based on the standard method, as described previously [15]. After separation by SDS-PAGE, proteins were transferred to Immobilon-P membrane (Millipore, USA) and incubated with MV-N-specific antibody. The membrane was then incubated with polyclonal antirabbit Igs/HRP (DakoCytomation, Denmark). Detection was car-

ried out using ECL Western blotting detection reagents (Amersham Biosciences, USA) and the LAS-1000UVmini-system (Fujifilm, Japan).

2.6 Electron microscopy (EM)

Each sample was spotted onto a 400 mesh copper grid (Maxtaform HF36; Pyser GSI, UK) coated with collodion, and was subjected to negative staining with 2% uranyl acetate. The samples were observed under an H-7000 electron microscope (Hitachi, Japan) as described elsewhere [16–18].

2.7 In-gel digestion of N protein by trypsin

Purified N protein was directly applied to a gel for 10% SDS-PAGE and stained with CBB as described above. A single band of approximately 60 kDa was excised from the gel and then destained five times with 50 mM NH_4HCO_3 in 50% methanol. After drying the gel in 100% ACN, 2.5 pmol of trypsin (Trypsin Gold Mass Spectrometry Grade, Promega) in 50 μL of 10 mM Tris (pH 8.5) was added, and in-gel digestion was carried out at 37°C for 16 h. Digested peptides were extracted by treating the gel twice with 0.1% TFA in 50% ACN and finally extracted once more by 0.1% TFA in 80% ACN for complete extraction.

2.8 MALDI-TOF/TOF MS analysis

Digested peptides were separated by nanoflow LC (Dina, KYA technologies, Japan). Each fraction was mixed with the matrix solution (5 mg/mL of CHCA and 60% ACN containing 0.1% TFA) and directly spotted onto a MALDI sample plate using a microfractionation system (AccuSpot, Shimadzu, Japan) for TOF-MS analysis. Peptide identification was carried out using a MALDI-TOF/TOF (4700 proteomics analyzer, Applied Biosystems, USA) as described previously [19, 20], followed by a database search using MASCOT ver. 2.0 (Matrix Science, UK) with maximum tolerance of 100 ppm in MS data and 0.15 Da in MS/MS data. The candidate peptide sequences were screened using probability-based MOWSE scores that exceeded their thresholds ($p<0.05$). The MS/MS spectra were interpreted using *DataExplorer* (Applied Biosystems).

2.9 ESI-Q-TOF MS analysis

Digested peptides were applied to a high-resolution nanoflow RP capillary LC (Dina, KYA technologies) coupled with an electrospray quadrupole TOF (ESI-Q-TOF) tandem mass spectrometer (Q-TOF-2, Micromass, UK) as described previously [21, 22]. The acquired MS/MS spectra were converted to text files of peak lists and processed using MASCOT ver. 2.0 (Matrix Science), with maximum tolerance of 100 ppm in MS data and 0.15 Da in MS/MS data, against each database. The candidate peptide sequences were screened using probability-based MOWSE scores that exceeded their thresholds ($p<0.05$).

2.10 Isolation of the C-terminal region from the core domain of N protein

Purified nucleocapsid, which formed a large herringbone structure, was treated with a high concentration of trypsin (0.1 mg/mL) at 37°C for 10 min in a buffer containing 150 mM NaCl and 20 mM Tris, and was immediately centrifuged at 70 000 rpm for 10 min in an Optima TL Ultracentrifuge with a TLA100.3 rotor (Beckman). The supernatant was collected and further incubated at 37°C for 1 h to completely digest the C-terminus for MS analysis. Digested peptides were then purified and concentrated using a ZipTipC18 column according to the manufacturer's instructions (Millipore). The resultant pellet after ultracentrifugation (consisting of the core domain of N) was analyzed by 10% SDS-PAGE.

2.11 Site-direct mutagenesis

Three mutant N plasmids (pS479A, pS510A, and pS479A/S510A) were produced by PCR-based mutagenesis. First, PCR amplification was performed by KOD Plus Ver. 2 (Toyobo) using the following primer pairs: S479A-F: 5′-ACTGCAGCAGAGTCAGGCCAAGATC-3′ (substituted nucleotides are underlined) and S479A-R (5′-phosphorylated): 5′-GTCAATGTCTAGGGGCATGCTGGTTG-3′, and S510A-F: GCAGACACGGACACCCCTAGGGTAT-3′ (substituted nucleotides are underlined) and S510A-R (5′-phosphorylated): 5′-GCCTTGTTCTTCCAAGATTCCTGCC-3′, using the pTNT vector (Promega) containing the ORF of N as template. After purification of the products using the MinElute PCR Purification Kit (Qiagen), each PCR product was ligated using T4 DNA Ligase (Promega). Using this fragment as a template, a second PCR was performed using forward and reverse primers for the pTNT vector. The final PCR products were digested using appropriate restriction enzymes and cloned into the pCAGGS expression vector. The double mutant (pS479A/S510A) was also produced by the same procedure.

2.12 Analysis of phosphorylation of mutant N by radioisotope

Cos-7 cells (5.0×10^5 cells) were transfected with 2 μg of the expression plasmid for wild-type (wt) N protein or phosphorylation site mutants, using FuGene 6 Transfection Reagent (Roche) as described above. One day after transfection, ^{32}P (phosphorus-32, PerkinElmer, USA) or ^{35}S (EXPRE^{35}S^{35}S Protein Labeling Mix, PerkinElmer) was added to the medium and cultured for further day. Then, the cells were lysed in lysis buffer containing 25 mM NaCl, 1% DOC, and 1% Triton X-100 at 4°C for 30 min, followed by clarification by centrifugation. mAb 8G against the N of canine distemper virus,

which shows crossreactivity with MV-N protein [23], and Protein A Sepharose™ CL-4B (Amersham Biosciences) were added to the supernatants and incubated at 4°C for 16 h with gentle rotation. After immunoprecipitation, samples were resolved by 10% SDS-PAGE. The amount of detected proteins were calculated using FLA-5100 (Fujifilm).

2.13 Synthesis of minigenomic RNA

To produce minigenomic RNA, both the 3′-leader and 5′-trailer sequences of the MV HL genome (nucleotide positions 1–107 and 15786–15894) and the ORF of the firefly luciferase gene cloned into pGL3-Basic vector (Promega) were amplified by *PfuTurbo*™ DNA polymerase (Stratagene, USA) using the following primers: HL-Leader-F: 5′-ACCAAACAAAGTTGGGTAAGGATAGATCAATCAATGATCA, HL-Leader-R: 5′-ATGTTTTTTGGCGTCTTCCATCTCGGATATCCCTAATCCTG, HL-Trailer-F: 5′-GCGGAAAGATCGCCGTGTAATAATTGGTTGAACTCCGGAACCC, HL-Trailer-R: 5′-ACCAGACAAAGCTGGGAATAGAAACTTCGTATTTTCAAAG, Luc-F: 5′-CAGGATTAGGGATATCCGAGATGGAAGACGCCAAAAACAT, and Luc-R: 5′-GGGTTCCGGAGTTCAACCAATTATTACACGGCGATCTTTCCGC. After purification of the PCR products from agarose gels, the fragments were joined by a second PCR using HL-Leader-F and HL-Trailer-R primers. The final PCR product was cloned into pMDB1 [24]. *In vitro* transcription was then performed using RiboMAX Large Scale RNA Production Systems (Promega) according to the manufacturer's instructions, and negative-strand minigenomic RNA was purified using MicroSpin G50 columns (Amersham Biosciences).

2.14 Minigenomic transcription assay

293 cells (1.5×10^5 cells) were transfected with 250 ng of the expression plasmid for wt N protein or mutants, together with 250 ng of the expression plasmid for P protein and 25 ng of the expression plasmid for L protein, using Lipofectamine™ LTX Reagent (Invitrogen). The following day, 500 ng of minigenomic RNA was transfected into the cells using Lipofectamine 2000 Reagent (Invitrogen). The cells were collected at 16 h post-transfection of RNA and lysed in 100 μL of Passive Lysis Buffer (Promega). Each 10 μL aliquot was mixed with 50 μL of PicaGene (Toyo Ink, Japan), and luciferase activity was determined by Lumat LB 9506 (Berthold, Germany). The experiment was performed in triplicate. Statistical analysis was performed by a one-way analysis of variance followed by Fisher's probable least squares difference test (StatWiew4.51.1, Abacus Concept, Canada).

2.15 N–P binding assay

The N, N mutants, and P were expressed in Cos-7 cells using FuGene 6 Transfection Reagent (Roche) as described above. After lysed in 250 μL of lysis buffer, the equal volume of lysate of N (or N mutants) and P were mixed and incubated for 30 min at 4°C. Solely expressed N and P were also lysed in 500 μL of lysis buffer and prepared as control. The supernatant of each sample was layered onto a discontinuous gradient containing 25, 30, and 40% w/w cesium chloride and was then centrifuged at 55 000 rpm for 30 min as described above. The band material that contained the N–P complex was collected and pelleted by ultracentrifugation at 70 000 rpm for 10 min. When solely expressed P was used, the same position with N band was collected. Each sample was then resolved by SDS-PAGE and detected by Western blotting using MV-N specific and MV-P specific antibodies.

3 Results and discussion

3.1 Purification of MV-N protein and electron microscopic observations

The N protein from the MV-HL strain was expressed in Cos-7 cells and the nucleocapsid was purified by cesium chloride density gradient centrifugation. As shown in Fig. 1, N protein, with a molecular weight of approximately 60 kDa, was clearly detected by CBB staining (Fig. 1a) and Western blot analysis using a specific antibody against MV-N (Fig. 1b). The structure of the purified nucleocapsid, which formed a typical large herringbone structure, was also observed by EM (Fig. 1c), indicating that N could be purified in its native form.

3.2 MALDI-TOF/TOF and ESI-Q-TOF MS analyses of full-length MV-N

First, to identify the phosphorylation sites of MV-N protein, full-length N protein was digested in SDS-PAGE gels by trypsin, and peptide identification was carried out using a

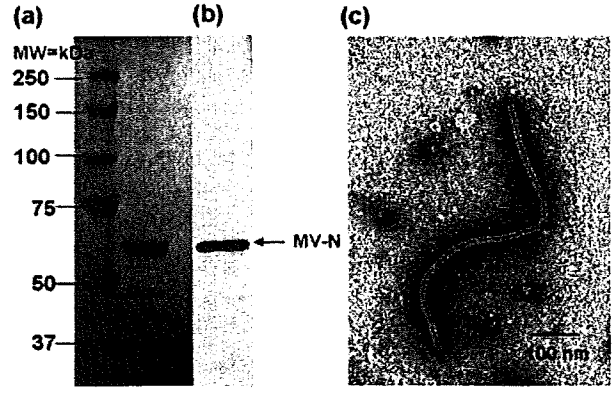

Figure 1. SDS-PAGE and Western blot analysis of purified N protein, and electron micrograph of negative-stained nucleocapsid structure. Recombinant N was expressed in Cos-7 cells and purified by cesium chloride density gradient centrifugation. (a) Samples were separated by 10% SDS-PAGE and detected by CBB or (b) Western blotting with MV-N-specific antibody. (c) Purified N protein was stained by 2% uranyl acetate and observed by EM. Bar represents 100 nm.

MALDI-TOF/TOF and an ESI-Q-TOF MS, followed by a database search with MASCOT ver. 2.0. As a result, 45 peptides that covered 57% of the sequence (Fig. 2a) and 54 peptides that covered 59% of the sequence (Fig. 2b) were identified, respectively. The total sequence coverage was 73%. Among the identified peptides, two remarkable peptides with m/z of 2931.2 and 2111.8 were found. When the increase in mass of 80-Da that corresponds to a phosphorylation (HPO_3) was calculated, the molecular masses of these peptides corresponded to the amino acid sequences at positions 464–490 and 498–516, respectively. We also determined intact N proteins in viral particles purified from MV-infected COBL-a cells using same procedure and detected the same possible phosphorylated peptides (data not shown) as those found on the recombinant N protein, indicating that phosphorylation sites of N protein are conserved in both transfected cells and MV-infected cells. In addition, MS/MS spectra of these precursor fragments showed a 98-Da neutral-loss of mass value corresponding to the H_3PO_4 ion. These results showed that each peptide contained a phosphorylated amino acid. However, we could not identify the phosphorylated amino acids because these peptides contained several possible phosphorylation sites and the MS/MS spectrum showed peaks with low intensity.

(a)MALDI-TOF-MS

```
  1 MATLLRSLAL FKRNKDKPPI TSGSGGAIRG IKHIIIVPIP GDSSITTRSR
 51 LLDRLVRLIG NPDVSGPKLT GALIGILSLF VESPGQLIQR ITDDPDVSIR
101 LLEVVQSDQS QSGLTFASRG TNMEDEADQY FSHDDPSNSD QSRSGWFENK
151 EISDIEVQDP EGFNMILGTI LAQIWVLLAK AVTAPDTAAD SELRRWIKYT
201 QQRRVVGEFR LERKWLDVVR NRIAEDLSLR RFMVALILDI KRTPGNKPRI
251 AEMIGDIDTY IVEAGLASFI LTIKFGIETM YPALGLHEFA GELSTLESLM
301 NLYQQMGETA PYMVILENSI QNKFSAGSYP LLWSYAMGVG VELENSMGGL
351 NFGRSYFDPA YFRLGQEMVR RSAGKVSSTL ASELGITAED ARLVSEIAMH
401 TTEDRISRAV GPRQAQVSFL HGDQSENELP GLGGKEDRRV KQGRGEAREN
451 YRETGSSRAS DARAAHPPTS MPLDIDTASE SGQDPQDSQR SADALLRLQA
501 MAGILEEQGS DTDTPRVYND RDLLD
```

(b)ESI-Q-TOF-MS

```
  1 MATLLRSLAL FKRNKDKPPI TSGSGGAIRG IKHIIIVPIP GDSSITTRSR
 51 LLDRLVRLIG NPDVSGPKLT GALIGILSLF VESPGQLIQR ITDDPDVSIR
101 LLEVVQSDQS QSGLTFASRG TNMEDEADQY FSHDDPSNSD QSRSGWFENK
151 EISDIEVQDP EGFNMILGTI LAQIWVLLAK AVTAPDTAAD SELRRWIKYT
201 QQRRVVGEFR LERKWLDVVR NRIAEDLSLR RFMVALILDI KRTPGNKPRI
251 AEMIGDIDTY IVEAGLASFI LTIKFGIETM YPALGLHEFA GELSTLESLM
301 NLYQQMGETA PYMVILENSI QNKFSAGSYP LLWSYAMGVG VELENSMGGL
351 NFGRSYFDPA YFRLGQEMVR RSAGKVSSTL ASELGITAED ARLVSEIAMH
401 TTEDRISRAV GPRQAQVSFL HGDQSENELP GLGGKEDRRV KQGRGEAREN
451 YRETGSSRAS DARAAHPPTS MPLDIDTASE SGQDPQDSQR SADALLRLQA
501 MAGILEEQGS DTDTPRVYND RDLLD
```

Figure 2. MALDI-TOF/TOF and ESI-Q-TOF MS analyses of MV-N protein. Digested peptides were separated by a nano-LC or a high-resolution nanoflow RP capillary LC and analyzed by (a) MALDI-TOF/TOF or (b) ESI-Q-TOF MS, followed by a database search using MASCOT v.2.0 (Matrix Science). Identified peptides are shown in bold.

3.3 Isolation of the C-terminal region of N protein

The N protein is mainly composed of two domains that span amino acid positions 1–400 (N-CORE) and 401–525 (N-TAIL). N-CORE is important for binding of N–N and N–RNA, and N-TAIL is required for interaction with P protein [25–28]. Although solely expressed N protein binds non-specifically to cellular RNA and forms a rigid herringbone structure, the C-terminal region is flexible and free to bind to the P protein [29–32]. Because the possible phosphorylation sites are located in the C-terminal region of the N protein, separation of the C-terminus from the core domain was performed. Purified nucleocapsid was treated briefly with a high concentration of trypsin, and the flexible C-terminal region was separated from the core domain. As the core domain formed a large herringbone structure in this condition, it was immediately precipitated by ultracentrifugation. As a result, the core domain of the N protein, with a molecular weight of approximately 45 kDa, was clearly detected in the pellet (Fig. 3, lane 2), indicating that the C-terminal region was successfully separated from the core domain and remained in the supernatant during ultracentrifugation.

3.4 MALDI-TOF/TOF MS analysis of the C-terminal region of the N protein

Purified C-termininal peptides of the N protein were separated by nano-LC and analyzed by MALDI-TOF/TOF MS. As shown in Fig. 4a, the MS/MS spectrum of the precursor fragment with an m/z of 2931.2 was analyzed. In this spectrum, five fragment ions, y12-98, y13-98, y14-98, y16-98, and y24-98, with a 98-Da neutral-loss of mass value corresponding to the H_3PO_4 ion, and eight fragment ions, y3, y6, y7, y8,

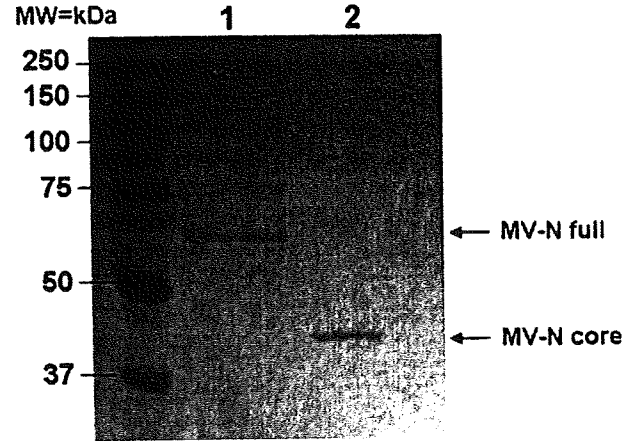

Figure 3. Isolation of the C-terminal region of N protein. Purified N-RNA complex was briefly treated with 0.1 mg/mL of trypsin and immediately centrifuged at 70 000 rpm for 10 min. The resultant pellet, which contained the core domain of the N protein, was resolved by 10% SDS-PAGE and stained with CBB. Lane 1: full-length N protein, lane 2: core domain of N protein with C-terminal region removed by trypsin treatment.

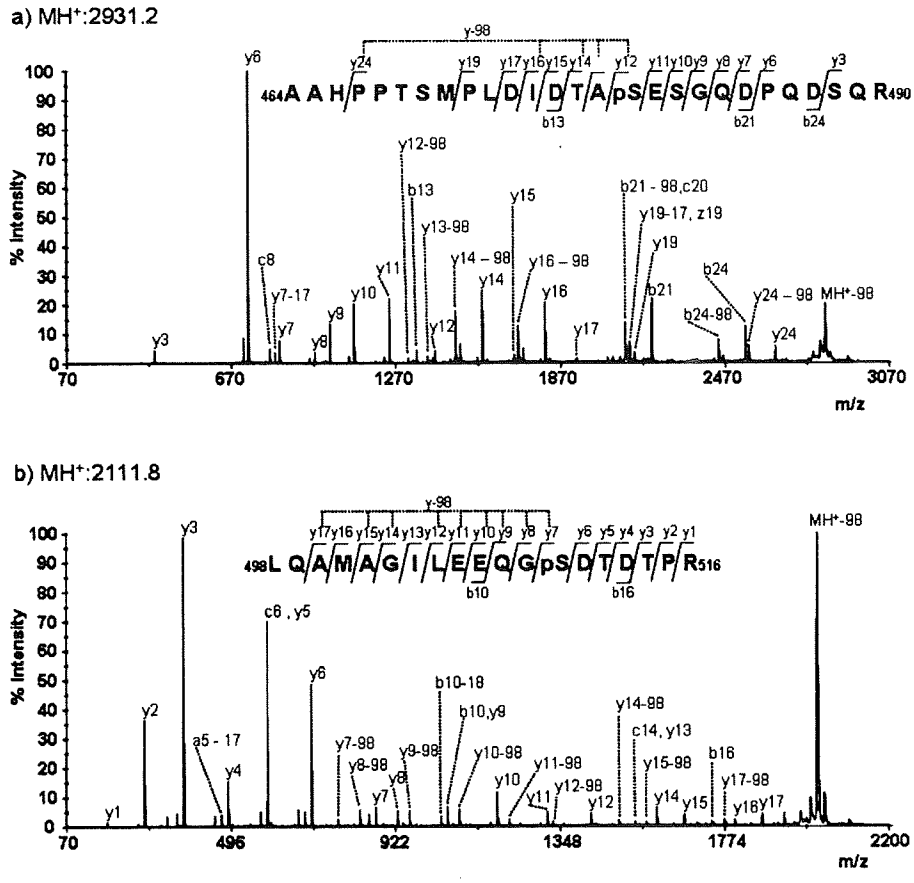

Figure 4. MALDI-TOF/TOF MS analysis of C-terminal peptides of MV-N protein. The spectrum was interpreted using the software *DataExplore*. The sequences from the N- and C-termini and the position of the modified residues were read based on b and y ions, respectively. (a) The MS/MS spectrum from the ion *m/z* 2931.2 (b) The MS/MS spectrum from the ion *m/z* 2111.8. A 98-Da neutral-loss of ion is shown above the sequences as y-98.

y9, y10, y11, and y12, with no loss of mass value, were observed. This indicated the amino acid sequence AAHPPTSMPLDIDTApSESGQDPQDSQR, which corresponds to amino acids 464–490 of the N protein phosphorylated at Ser479. Figure 4b shows the MS/MS spectrum of the precursor fragment with an *m/z* of 2111.8. In this spectrum, all fragment ions from y1 to y17, with no loss of mass value, and nine fragment ions, y7-98, y8-98, y9-98, y10-98, y11-98, y12-98, y14-98, y15-98, and y17-98, with a 98-Da neutral-loss ion, were clearly detected. This indicated that the amino acid sequence LQAMAGILEEQGpSDTDTPR corresponds to amino acids 498–516 of the N protein phosphorylated at Ser510.

Similar results were obtained when an alternative MS/MS system was used. Purified C-terminal peptides were applied to a high-resolution nanoflow RP capillary LC coupled with an ESI-Q-TOF MS, and it was confirmed that the same regions were phosphorylated (data not shown). These results led to the conclusion that S479 and S510 of the MV-N were phosphorylated.

On homologous search of amino acid sequence of N gene using blast program, these two sites were completely conserved among 100 MV strains including many recent field isolates such as Ichinose, San Diego, and Chicago [33, 34]. In addition, these two sites were conserved in other laboratory passaged or vaccine strains [35], although there were many substitutions in C-terminal region, suggesting that phosphorylation of these sites have important function (s) in MVs. A previous study suggested that the N protein of MV Nagahata strain contained five phosphorylation sites although their positions were not determined [9]. By comparison of amino acid sequence of N protein between Nagahata and our HL strains, eleven mutations of S or T have been observed although the two sites identified in the present study were conserved, suggesting that these differences might affect the number of phosphorylation sites of the N protein. However, the efficiency of ionization of phosphorylated peptides is inherently low compared with unmodified peptides, therefore it is sometimes difficult to detect such peptides. In addition, it is difficult to cover the whole sequence of a protein in TOF-MS analysis. Therefore, the possibility that one or more additional phosphorylation sites exist in the N protein of HL strain could not be excluded.

3.5 Determination of phosphorylation of mutant N proteins

To confirm that the serine residues at 479 and 510 are phosphorylated, we constructed N protein mutants in which these serine residues were replaced by alanine. Three

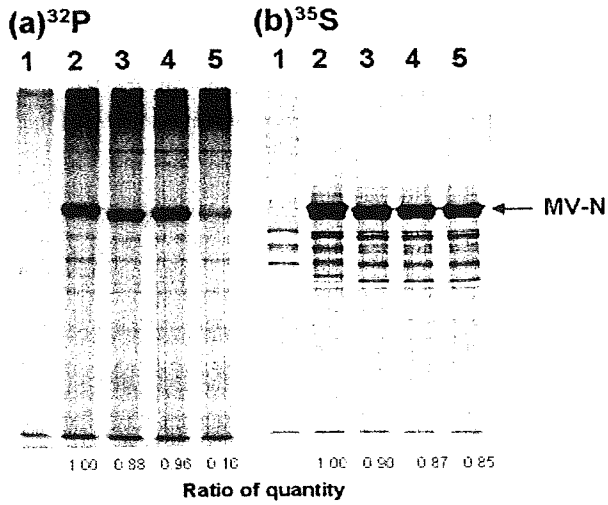

Figure 5. Radioisotope labeling and immunoprecipitation of mutant N proteins. Wt N protein and three mutants were expressed in Cos-7 cells and labeled with (a) ^{32}P or (b) ^{35}S. After immunoprecipitation by antibody, samples were resolved by 10% SDS-PAGE and detected by FLA-5100. Lane 1: Cos-7 cells, lanes 2–5: wt N-, S479A- S510A-, and S479A/S510A-expressing Cos-7 cells, respectively. Ratio of quantity of each sample against wt N was labeled on the bottom of each lane.

mutants (S479A, S510A, and S479A/S510A) and wt N were expressed in Cos-7 cells in the presence of ^{32}P or ^{35}S, and phosphorylation of the mutant N proteins was analyzed. Strong labeling with ^{32}P was observed in wt, S479A and S510A (Fig. 5a, lanes 2–4), whereas the intensity was dramatically reduced in S479A/S510A (Fig. 5a, lane 5), although all four N proteins were detected in almost equal amounts by ^{35}S labeling (Fig. 5b). These results showed that S479 and S510 are the major phosphorylation sites of the N protein.

3.6 Effect of phosphorylation on transcription of minigenomic RNA

Because the RNP that is assembled by the N, P, and L proteins, together with RNA containing both the 5′ and 3′ promoter regions of the viral genome, has the ability to replicate and transcribe mRNA [36], RNPs formed by the phosphorylation mutants of N protein are useful tools for investigation of the effect of phosphorylation on transcription and replication. Therefore, we developed a minigenomic assay system for MV-HL using negative-strand luciferase RNA flanked by both promoters, and determined the transcriptional activity of the mutant N proteins. Both S479A and S510A showed approximately 20% luciferase activity, and S479A/S510A showed approximately 40% activity, compared with wt N (Fig. 6). To examine whether the low transcriptional activity was due to the lower expression rate of the mutant N protein in the transfection cells or not, we measured the amount of the N and N mutant proteins after those plasmids were transfected. We observed that expression rate was not different from each other (approximately 90%). Thus, the suppression of transcriptional activity is not due to the amount of the mutant N protein expressed in the cells. These results indicate that the loss of phosphorylation of the N protein downregulates transcriptional activity.

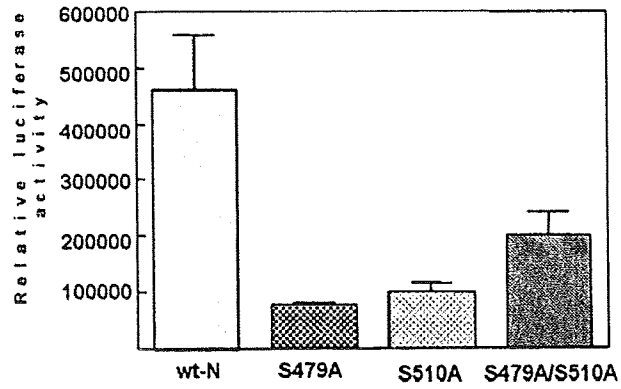

Figure 6. Minigenomic transcription assay. Negative-strand minigenomic RNA containing the ORF of luciferase gene was transfected into 293 cells expressing wt or mutant N protein together with P and L proteins. Luciferase activities of cell extracts were measured using Lumat LB 9506. Statistical analysis was performed using the software StatWiew4.51.1, (Abacus concept).

The reason for the partial recovery of luciferase activity that was observed in the double mutant (S479A/S510A) is not clear, however, this result supported the conclusion that downregulation observed in each single mutation was not caused by structural changes related to replacement of the amino acid Ser with Ala.

3.7 Binding ability of mutant N with P protein

One of the functions of the N protein is to support replication and transcription, together with the P and L proteins. As the C-terminal region is required for interaction with the P protein [25, 26, 28], we analyzed the binding ability of wt N and N mutants with P protein using the CsCl purification method of nucleocapsid. As a result, wt N and all mutant N proteins strongly interacted to P protein and P was purified as N–P complex (Fig. 7, lanes 3–6). These results indicated that low transcriptional activity of mutant N may not due to loss of binding activity with P protein but that some of host protein (s) may be implicated in transcriptional activity. Further *in vivo* study using reverse genetics system of MV may clarify the mechanism of upreguration of transcriptional activity by phosphorylation.

4 Concluding remarks

In the present study, we purified the C-terminal peptides of expressed N protein, and identified two major phosphorylation sites, at positions S479 and S510, using two types of

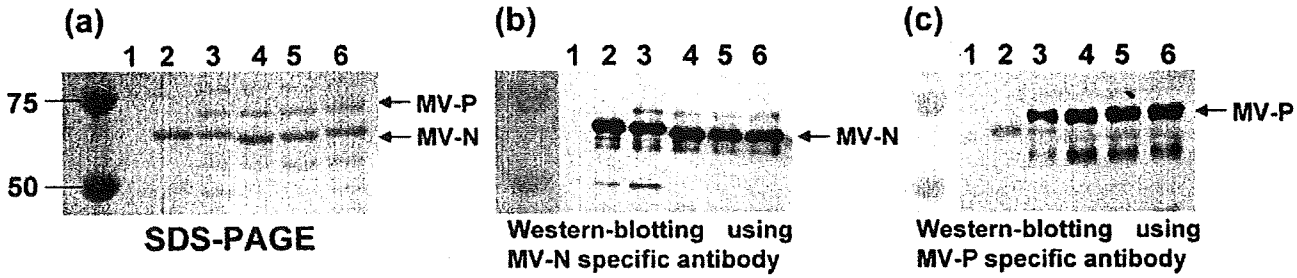

Figure 7. N–P binding assay. MV-N, N mutants, and P proteins were expressed in Cos-7 cells. After mixed the cell extract of N (or N mutants) and P, N–P complex was purified by cesium chloride density gradient centrifugation. (a) Each sample was then resolved by SDS-PAGE, (b) detected by Western blotting using MV-N specific, and (c) MV-P specific antibodies. Lanes 1:solely expressed P, lanes 2:solely expressed N, lanes 3: N + P, lanes 4: S479A + P, lanes 5: S510A + P, lanes 6: S479AS510A + P.

TOF-MS. This is the first report of identification of phosphorylation sites of an N protein in the family *Paramyxoviridae*. As the purification and manipulation of highly concentrated intact viruses requires specialized facilities and skills, especially when using deadly viruses, this proteomic approach is considered to be very safe and useful for researchers to identify and investigate the role of PTM of N proteins of viruses of the family *Paramyxoviridae*.

In the minigenomic assay, all three mutants (S479A, S510A, and S479A/S510A) showed approximately 20–40% luciferase activity compared with wt N protein, suggesting that phosphorylation of N protein is not essential but plays an important role in activation of transcription of viral mRNA and/or replication of genome *in vivo*. The N protein of MV has multiple functions [37–42]. Since the N proteins of other paramyxoviruses have similar structure and functions, the phosphorylation is suggested to provide important functions commonly in replication of paramyxoviruses.

This study was supported by a grant from the Program for Promotion of Basic Research Activities for Innovative Biosciences (PROBRAIN) and a grant-in-aid from the Ministry of Education, Science, Culture, and Sports, Japan.

The authors have declared no conflict of interest.

5 References

[1] Lamb, R. A., Kolakofsky, D., in: Knipe, D. M., Howley, P. M. (Eds.), *Fields Virology, Paramyxoviridae*, Lippincott, Williams and Wilkins, Philadelphia 2001, pp. 1305–1340.

[2] Griffin, D. E., in: Knipe, D. M., Howley, P. M. (Eds.), *Fields Virology, Measles Virus*, Lippincott, Williams and Wilkins, Philadelphia 2001, pp. 1401–1441.

[3] Bellini, W. J., Englund, G., Rozenblatt, S., Arnheiter, H. *et al.*, Measles virus P gene codes for two proteins. *J. Virol.* 1985, *53*, 908–919.

[4] Cattaneo, R., Kaelin, K., Baczko, K., Billeter, M. A., Measles virus editing provides an additional cystein-rich protein. *Cell* 1989, *56*, 759–764.

[5] Warnes, A., Fooks, A. R., Dowsett, A. B., Wilkinson, G. W. G. *et al.*, Expression of the measles virus nucleoprotein gene in *Escherichia coli* and assembly of nucleocapsid-like structures. *Gene* 1995, *160*, 173–178.

[6] Das, T., Schuster, A., Schneider-Schaulies, S., Banerjee, A. K., Involvement of cellular casein kinase II in the phosphorylation of measles virus P protein: Identification of phosphorylation sites. *Virology* 1995, *211*, 218–226.

[7] Liu, Z., Huntley, C. C., De, B. P., Das, T. *et al.*, Phosphorylation of canine distemper virus P protein by protein kinase C-zeta and casein kinase II. *Virology* 1997, *232*, 198–206.

[8] Ofir, R., Weinstein, Y., Bazarsky, E., Blagerman, S. *et al.*, Tyrosine phosphorylation of measles virus nucleocapsid protein in persistently infected neuroblastoma cells. *Virus Genes* 1996, *13*, 203–210.

[9] Gombart, A. F., Hirano, A., Wong, T. C., Nucleoprotein phosphorylated on both serine and threonine is preferentially assembled into the nucleocapsids of measles virus. *Virus Res.* 1995, *37*, 63–73.

[10] Segev, Y., Ofir, R., Salzberg, S., Heller, A. *et al.*, Tyrosine phosphorylation of measles virus nucleocapsid protein in persistently infected neuroblastoma cells. *J. Virol.* 1995, *69*, 2480–2485.

[11] Kobune, F., Ami, Y., Katayama, M., Takahashi, M. *et al.*, A novel monolayer cell line derived from human umbilical cord blood cells shows high sensitivity to measles virus. *J. Gen. Virol.* 2007, *88*, 1565–1567.

[12] Kobune, F., Takahashi, H., Terao, K., Ohkawa, T. *et al.*, Nonhuman primate models of measles. *Lab. Anim. Sci.* 1996, *46*, 315–320.

[13] Sato, H., Kobune, F., Ami, Y., Yoneda, M. *et al.*, Immune responses against measles virus in cynomolgus monkeys. *Comp. Immun. Microbiol. Infect. Dis.* 2007, *31*, 25–35.

[14] Tokui, M., Takei, I., Tashiro, F., Shimada, A. *et al.*, Intramuscular injection of expression plasmid DNA is an effective means of long-term systemic delivery of interleukin-5. *Biochem. Biophys. Res. Commun.* 1997, *233*, 527–531.

[15] Hagiwara, K., Tomita, M., Nakai, K., Kobayashi, J. *et al.*, Determination of the nucleotide sequence of *Bombyx mori* cytoplasmic polyhedrosis virus segment 9 and its expression in BmN4 cells. *J. Virol.* 1998, *72*, 5762–5768.

[16] Hagiwara, K., Naitow, H., Assembly into single-shelled virus-like particles by major capsid protein VP1 encoded by genome segment S1 of *Bombyx mori* cypovirus 1. *J. Gen. Virol.* 2003, *84*, 2439–2441.

[17] Hagiwara, K., Higashi, T., Namba, K., Uehara-Ichiki, T. *et al.*, Assembly of single-shelled cores and double-shelled virus-like particles after baculovirus expression of major structural proteins P3, P7 and P8 of *Rice dwarf virus*. *J. Gen. Virol.* 2003, *84*, 981–984.

[18] Hagiwara, K., Higashi, T., Miyazaki, N., Naitow, H. *et al.*, The amino-terminal region of major capsid protein P3 is essential for self-assembly of single-shelled core-like particles of *Rice dwarf virus*. *J. Virol.* 2004, *78*, 3145–3148.

[19] Takada, R., Satomi, Y., Kurata, T., Ueno, N. *et al.*, Monounsaturated fatty acid modification of Wnt protein: Its role in Wnt secretion. *Dev. Cell* 2006, *11*, 791–801.

[20] Akita, Y., Kawasaki, H., Imajoh-Ohmi, S., Fukuda, H. *et al.*, Protein kinase Cε phosphorylates keratin 8 at Ser8 and Ser23 in GH4C1 cells stimulated by thyrotropin-releasing hormone. *FEBS*, 2007, *274*, 3270–3285.

[21] Oyama, M., Kozuka-Hata, H., Suzuki, Y., Semba, K. *et al.*, Diversity of translation start sites may define increased complexity of the human short ORFeome. *Mol. Cell. Proteomics* 2007, *6*, 1000–1006.

[22] Oyama, M., Itagaki, C., Hata, H., Suzuki, Y. *et al.*, Analysis of small human proteins reveals the transcription of upstream open reading frames of mRNAs. *Genome Res.* 2004, *14*, 2048–2052.

[23] Masuda, M., Sato, H., Kamata, H., Katsuo, T. *et al.*, Characterization of monoclonal antibodies directed against the canine distemper virus nucleocapsid protein. *Comp. Immunol. Microbiol. Infect. Dis.* 2006, *29*, 157–165.

[24] Baron, M. D., Barrett, T., Rescue of rinderpest virus from cloned cDNA. *J. Virol.* 1997, *71*, 1265–1271.

[25] Bankamp, B., Horikami, S. M., Thompson, P. D., Huber, M. *et al.*, Domain of the measles virus N protein required for binding to P protein and self-assembly. *Virology* 1996, *216*, 272–277.

[26] Liston, P., Batal, R., DiFlumeri, C., Briedis, D. J., Protein interaction domains of the measles virus nucleocapsid protein (NP). *Arch. Virol.* 1997, *142*, 305–321.

[27] Karlin, D., Longhi, S., Canard, B., Substitution of two residues in the measles virus nucleoprotein results in an impaired self-association. *Virology* 2002, *302*, 420–432.

[28] Johansson, K., Bourhis, J. M., Campancci, V., Cambillau, C. *et al.*, Crystal structure of the measles virus phosphoprotein domain responsible for the induced folding of the C-terminal domain of the nucleoprotein. *J. Biol. Chem.* 2003, *278*, 44567–44573.

[29] Karlin, D., Ferron, F., Canard, B., Longhi, S., Structural disorder and modular organization in *Paramyxoviridae* N and P. *J. Gen. Virol.* 2003, *84*, 3239–3252.

[30] Longhi, S., Receveur-Brechot, V., Karlin, D., Johansson, K. *et al.*, The C-terminal domain of the measles virus nucleoprotein is intrinsically disordered and folds upon binding to the C-terminal moiety of the phosphoprotein. *J. Biol. Chem.* 2003, *278*, 18638–18648.

[31] Schoehn, G., Mavrakis, M., Albertini, A., Wade, R. *et al.*, The 12Å structure of trypsin-treated measles virus N-RNA. *J. Mol. Biol.* 2004, *339*, 301–312.

[32] Bhella, D., Ralph, A., Yeo, R. P., Conformational flexibility in recombinant measles virus nucleocapsids visualized by cryo-negative stain electron microscopy and real-space helical reconstruction. *J. Mol. Biol.* 2004, *340*, 319–331.

[33] Takeuchi, K., Miyajima, N., Kobune, F., Tashiro, M., Comparative nucleotide sequence analyses of the entire genomes of B95a cell-isolated and vero cell-isolated measles viruses from the same patient. *Virus Genes* 2000, *20*, 253–257.

[34] Rota, P. A., Bloom, A. E., Vanchiere, J. A., Bellini, W. J., Evolution of the nucleoprotein and matrix genes of wild-type strains of measles virus isolates from recent epidemics. *Virology* 1994, *198*, 724–730.

[35] Kreis, S., Vardas, E., Whistler, T., Sequence analysis of the nucleocapsid gene of measles virus isolates from South Africa identifies a new genotype. *J. Gen. Virol.* 1997, *78*, 1581–1587.

[36] Brown, D. D., Collins, F. M., Duprex, W. P., Baron, M. D. *et al.*, 'Rescue' of mini-genomic constructs and viruses by combinations of morbillivirus N, P and L proteins. *J. Gen. Virol.* 2005, *86*, 1077–1081.

[37] Ravanel, K., Castelle, C., Defrance, T., Wild, T. F. *et al.*, Measles virus nucleocapsid protein binds to FcgammaRII and inhibits human B cell antibody production. *J. Exp. Med.* 1997, *186*, 269–278.

[38] Marie, J. C., Kehren, J., Trescol-Biemont, M. C., Evlashev, A. *et al.*, Mechanism of measles virus-induced suppression of inflammatory immune responses. *Immunity* 2001, *14*, 69–79.

[39] Marie, J. C., Saltel, F., Escola, J. M., Jurdic, P. *et al.*, Cell surface delivery of the measles virus nucleoprotein: A viral strategy to induce immunosuppression. *J. Virol.* 2004, *78*, 11952–11961.

[40] TenOever, B. R., Servant, M. J., Grandvaux, N., Lin, R. *et al.*, Recognition of the measles virus nucleocapsid as a mechanism of IRF-3 activation. *J. Virol.* 2002, *76*, 3659–3669.

[41] Zhang, X., Glendening, C., Linke, H., Parks, C. L. *et al.*, Identification and characterization of a regulatory domain on the carboxyl terminus of the measles virus nucleocapsid protein. *J. Virol.* 2002, *76*, 8737–8746.

[42] Sato, H., Masuda, M., Kanai, M., Tsukiyama-Kohara, K. *et al.*, Measles virus N protein inhibits host translation by binding to eIF3-p40. *J. Virol.* 2007, *81*, 11569–11576.

Available online at www.sciencedirect.com
ScienceDirect
Comparative Immunology, Microbiology and Infectious Diseases 32 (2009) 29–41
COMPARATIVE IMMUNOLOGY MICROBIOLOGY & INFECTIOUS DISEASES
www.elsevier.com/locate/cimid

Inhibition of host protein synthesis in B95a cells infected with the HL strain of measles virus

Yoshihisa Inoue [a], Kyoko Tsukiyama-Kohara [b], Misako Yoneda [a], Hiroki Sato [a], Chieko Kai [a,*]

[a] *Laboratory Animal Research Center, The Institute of Medical Science, The University of Tokyo, 4-6-1 Shirokanedai Minato-ku, Tokyo 108-8639, Japan*
[b] *Department of Experimental Phylaxiology, Faculty of Medical and Pharmaceutical Sciences, Kumamoto University, 1-1-1 Honjo Kumamoto, Kumamoto 860-8556, Japan*

Accepted 9 August 2008

Abstract

The shut-off of host protein synthesis in virus-infected cells is one of the important mechanisms for viral replication. In this report, we showed that the HL strain of measles virus (MeV-HL) as well as other field isolates, which were isolated from human blood lymphocytes using B95a cells, induce the shut-off in B95a cells. Since the Edmonston strain of MeV failed to induce the shut-off in B95a cells, the ability to induce the shut-off was considered to be dependent on virus strains. Although, the modification of eukaryotic translation initiation factors (eIF) including eIF4G, eIF4E, and 4E-BP1 was reported for shut-off by various viruses, the involvement of these eIFs was not observed in MeV-HL-infected B95a cells. Instead, the accumulation of phosphorylated eIF2α was found to coincide to the decrease of host protein synthesis, suggesting the involvement of phosphorylation of eIF2α in inhibition of translation as one of the mechanisms of the shut-off.

Keywords: Measles virus; Shut-off; eIF2α

Résumé

La suppression de la synthèse protéique de la cellule hôte au cours de l'infection est un des mécanismes majeurs de la réplication virale. Dans cette étude nous avons montré que la souche HL du virus de la rougeole (MeV-HL) ainsi que d'autres souches sauvages du virus, isolées dans

* Corresponding author. Tel.: +81 3 5449 5497; fax: +81 3 5449 5379.
E-mail address: ckai@ims.u-tokyo.ac.jp (C. Kai).

0147-9571/$ – see front matter © 2008 Elsevier Ltd. All rights reserved.
doi:10.1016/j.cimid.2008.08.007

des cellules B95a à partir de lymphocytes sanguins humains, induisent ce type de suppression dans les cellules B95a. Comme la souche Edmonston du virus de la rougeole est incapable d'induire cette suppression dans les cellules B95a, cette propriété a été considérée comme dépendante de la souche virale. Bien qu'il ait été observé une extinction de l'expression des facteurs d'initiation de la traduction eucaryote (eIF) dont eIF4G, eIF4E et 4E-BP1 par de nombreux virus, il n'a pas été vu d'implication de ces facteurs dans les cellules B95a infectées par MeV-HL. Par contre, dans ces cellules on a montré que l'accumulation de la forme phosphorylée de eIF2a est concomitante à la diminution de la synthèse protéique, suggérant l'inhibition de la traduction par phosphorylation de eIF2a dans pourrait être un des mécanismes de la suppression de la synthèse protéique.

Mots clés : virus de la rougeole ; eIF2α ; suppression de la synthèse protéique

1. Introduction

One of the most striking changes observed in the cells infected with certain viruses is the almost complete inhibition of the translation of host mRNAs in the presence of effective translation of viral mRNAs [1]. Such inhibition of host protein synthesis (shut-off) have been reported in the infection with picornaviruses, adenovirus, influenza virus and vesicular stomatitis virus (VSV) and considered to occur at the stage of host translational level, as cellular mRNAs are recovered as an intact and functionally active form from the virus-infected cells [2–5]. Modification of eukaryotic initiation factors (eIFs) including the subunit of eIF4F complex (e.g., eIF4G and eIF4E) is observed in these virus-infected cells [6], and the modification of eIF4F by the viral infection resulting in the inhibition of cap-dependent translation is proposed as one of the mechanisms for shut-off.

Measles virus (MeV) belongs to the genus *Morbillivirus* within the family Paramyxoviridae, the genome of which is a single-stranded RNA with negative polarity. The MeV mRNA has a cap structure at 5′ end of the mRNA and is thought to be translated in a cap-dependent manner [7]. The Edmonston strain of MeV (MeV-Ed) has been reported not to induce the host shut-off of host protein synthesis [8,9]. Although most information on MeV–cell interaction has been obtained from the studies on MeV-Ed in epithelial or epithelial-like cells such as CV-1, Hela and Vero cells, accumulating evidence obtained by the use of lymphoblastoid B95a cells has suggested that MeV circulating in human is heterogenous and MeV-Ed represent minor subpopulation of the virus selected during long passage in cell cultures [10].

In the present study, we examined the effect of the HL strain of MeV (MeV-HL), which was isolated using B95a cells from a measles patient and maintains virulence in monkeys [10], on the host protein synthesis in B95a cells and found that MeV-HL induces marked shut-off of host protein synthesis. As the mRNA level of host proteins was not altered in MeV-HL-infected B95a cells, we focused on possible modification of translation factors involved in the cap-dependent translation initiation to clarify the mechanisms involved in the induction of the shut-off of host protein synthesis by MeV-HL infection.

2. Materials and methods

2.1. Cell and viruses

B95a cells [11] were grown in RPMI1640 supplemented with 5% fetal calf serum (FCS). As a typical virus isolated from measles patient, MeV-HL and two other field isolates, 9106 and 9301 strains [12] were used. MeV-Ed that was passed twice in B95a cells was also used. Virus infectivity titers were determined in B95a cells and expressed as a 50% tissue culture infectious dose ($TCID_{50}$). For examining shut-off of host protein synthesis, a monolayer culture of B95a cells was infected with MeV with a multiplicity of infection (MOI) of 1 $TCID_{50}$.

2.2. Metabolic labeling of cells

B95a cells were mock-infected or infected with MeV and then labeled with [^{35}S] EXPRESS (PerkinElmer, MA, USA) in methionine- and cystein-free RPMI1640 with 2% FCS for 1 h at 0, 11, 17, 23 and 35 h post-infection (hpi). Cells were lysed in lysis buffer C (125 mM NaCl, 20 mM Tris–HCl pH 8.0, 0.5% NP-40). Cell lysates were centrifuged and the supernatants were collected. Proteins were electrophoresed in SDS-PAGE gels, and ^{35}S-labeled proteins were visualized with autoradiography using X-ray film or quantitated with a phosphoimager plate in BAS 2000 (Fujifilm, Tokyo, Japan).

2.3. Real-time RT-PCR

Real-time RT-PCR was used to determine the expression level of glyceraldehyde-3-phosphate dehydrogenase (GAPDH) mRNA and 18S rRNA in accordance with the method described by Sato et al. [13].

2.4. Antibodies

Rabbit polyclonal antibodies against eIF4G and eIF2α, goat polyclonal antibodies against phospho-eIF4E, 4E-BP1 and β-actin and mouse monoclonal antibody against eIF4E were purchased from Santa Cruz Biotechnology, Inc. (CA, USA). Rabbit polyclonal antibody against phospho-eIF2α was purchased from Cell Signaling Technology (MA, USA). Horseradish peroxidase-conjugated secondary antibodies against rabbit, goat or mouse immunoglobulin were purchased from DAKO (Glostrup, Denmark).

2.5. Western blotting assay

Mock- or MeV-HL-infected B95a cells were lysed with lysis buffer C containing 1 mM PMSF, 1 mM benzamidine, 1 μg/ml aprotinine, 100 μM NaF and 1 μM Na_3VO_4. Equal amounts of protein extracts were subjected to SDS-PAGE and the proteins were transferred onto Hybond-N(+) nitrocellulose membrane (GE Healthcare UK Ltd., Buckinghamshire, UK). Detection of 4E-BP1 was performed as described previously [14]. Western blotting assay was performed with each antibody according to the recommendations of

manufacturer. Bands were visualized using an ECL plus detection reagent (GE Healthcare UK Ltd.). The intensity of bands was quantitated by scanning with LAS-1000 mini and Imagegauge software (Fujifilm).

2.6. Establishment of cell lines stably expressing eIF2α

Human eIF2α cDNA was obtained with PCR using the sense primer (5′-GCGGGAATCACACACATACCTCAGAA-3′) and antisense primer (5′-TCAAGTCTAG-GATTTACAGCCAGGAAGCGC-3′) with reverse transcription (RT) products from the mRNA of HeLa cells and was then subcloned into pCR2.1-TOPO vector (Invitrogen, CA, USA). Phosphorylation site at serine 51 of eIF2α cDNA was mutated to alanine (S51A) using a PCR-based mutagenesis strategy with Pfu turbo polymerase (Stratagene, CA, USA) to obtain the cDNA of S51A mutant eIF2α. The eIF2α cDNA was inserted into a pCMV-myc expressing vector (Clontech, CA, USA). The myc-tagged eIF2α (wild type or S51A mutant) expression vector (1.5 μg) and 0.5 μg of pCDNA3.1 (Invitrogen) were co-transfected to B95a cells with DMRIE-C reagent (Invitrogen) according to the recommendations of manufacturer. After incubation for 24 h, the cells were replated to 150-mm dishes and cultured in RPMI1640 with 5% FCS and 500 μg/ml G418 (bioactive; Invitrogen). G418-resistant colonies were selected approximately 2 weeks later. Expression of myc-tagged proteins was confirmed by Western blotting assay using a monoclonal antibody against myc tag (Clontech).

3. Results

3.1. Effect of several strains of MeV on host protein synthesis in B95a cells

Effect of MeV-HL-infection on protein synthesis was shown in Fig. 1a. The rate of host protein synthesis was determined by quantitation of the total radioactivity of one lane except four bands of N, P, M and H derived from MeV-HL. The ratio of host protein synthesis in MeV-HL-infected B95a cells to that in mock-infected cells was shown in Fig. 1b. The relative rate of viral protein synthesis to host protein synthesis, which was determined by sum of the radioactivity of four viral proteins and that of host proteins, was also shown in Fig. 1b. A marked decrease of host protein synthesis was observed between 18 and 36 hpi. On the other hand, relative viral protein synthesis to host protein synthesis increased and reached a peak at 24 hpi. This result indicates that MeV-HL induces shut-off of host protein synthesis in B95a cells.

Subsequently, other field isolates of MeV, 9106 strain and 9301 strain were also examined for their ability to induce the shut-off (Fig. 2a right). The autoradiograph gel was stained with Coomassie brilliant blue before drying the gel to confirm that total protein levels are equal (Fig. 2a left). As shown in Fig. 2a, 9106 and 9301 strains also induced the inhibition of host protein synthesis at 24 hpi similar to MeV-HL. The effect of the MeV-Ed, which was reported not to induce shut-off in CV-1 or Hela cells, was tested in B95a cells. Host protein synthesis in MeV-Ed-infected B95a cells was not inhibited until 24 hpi when the inhibition was clearly observed in MeV-HL-infected cells (Fig. 2b). These results